Research Article
Experimental and Translational Hepatology

JOURNAL
OF HEPATOLOGY

Activation and transcriptional profile of monocytes and CD8$^+$ T cells are altered in checkpoint inhibitor-related hepatitis

Graphical abstract

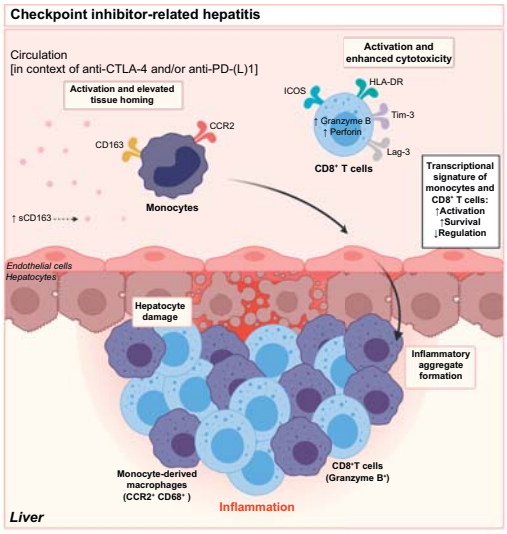

Highlights

- CPI-Hepatitis is associated with peripheral monocyte activation (CD163^{hi}, CCR2^{hi}).
- Peripheral CD8 T cells in CPI-Hepatitis showed elevated activation/cytotoxicity.
- Liver immunohistochemistry showed CD8 T cell/macrophage aggregates in CPI-Hepatitis.
- Monocyte-derived macrophages from CPI-Hepatitis show enhanced cytokine secretion *in vitro*.

Authors

Cathrin L.C. Gudd, Lewis Au, Evangelos Triantafyllou, …, Charalambos G. Antoniades, Samra Turajlic, Lucia A. Possamai

Correspondence

l.possamai@imperial.ac.uk
(L.A. Possamai).

Lay summary

Some patients who receive immunotherapy for cancer develop liver inflammation, which requires cessation of cancer treatment. Herein, we describe ways in which the white blood cells of patients who develop liver inflammation differ from those of patients who receive the same immunotherapy but do not experience liver-related side effects. Targeting some of the pathways we identify may help to prevent or manage this side effect and facilitate cancer treatment.

https://doi.org/10.1016/j.jhep.2021.02.008
 J. Hepatol. 2021, 75, 177–189

Research Article
Experimental and Translational Hepatology

JOURNAL OF HEPATOLOGY

Activation and transcriptional profile of monocytes and CD8$^+$ T cells are altered in checkpoint inhibitor-related hepatitis

Cathrin L.C. Gudd[1], Lewis Au[2], Evangelos Triantafyllou[1], Benjamin Shum[2], Tong Liu[1], Rooshi Nathwani[1], Naveenta Kumar[1], Sujit Mukherjee[1], Ameet Dhar[1], Kevin J. Woollard[3], You Yone[4], David J. Pinato[4], Mark R. Thursz[1], Robert D. Goldin[1], Martin E. Gore[2], James Larkin[2], Wafa Khamri[1,†], Charalambos G. Antoniades[1,†], Samra Turajlic[2,†], Lucia A. Possamai[1,*,†]

[1]*Department of Metabolism, Digestion & Reproduction, Imperial College London, London, UK;* [2]*Renal and Skin Units, The Royal Marsden Hospital National Health Service Foundation Trust, London, UK;* [3]*Department of Immunology and Inflammation, Imperial College London, London, UK;* [4]*Department of Surgery & Cancer, Faculty of Medicine, Imperial College London, London, UK*

Background & Aims: Checkpoint inhibitor-related hepatitis (CPI-Hep) is an emerging clinical challenge. We aimed to gain insights into the immunopathology of CPI-Hep by comprehensively characterising myeloid and lymphoid subsets.

Methods: CPI-treated patients with or without related hepatitis (CPI-Hep; n = 22 and CPI-noHep; n = 7) were recruited. Phenotypic and transcriptional profiling of peripheral immune subsets was performed and compared with 19 healthy controls (HCs). *In vitro* monocyte-derived macrophages (MoMFs) were assessed for activation and cytokine production. CD163, CCR2, CD68, CD3, CD8 and granzyme B expression was assessed using immunohistochemistry/immunofluorescence (n = 4).

Results: A significant total monocyte depletion was observed in CPI-Hep compared with HCs (p = 0.04), along with a proportionate increase in the classical monocyte population (p = 0.0002) and significant upregulation of CCR2, CD163 and downregulation of CCR7. Soluble CD163 levels were significantly elevated in CPI-Hep compared with HCs (p <0.0001). *In vitro* MoMFs from CPI-Hep showed enhanced production of pro-inflammatory cytokines. CD8$^+$ T cells demonstrated increased perforin, granzyme B, ICOS and HLA-DR expression in CPI-Hep. Transcriptional profiling indicated the presence of activated monocyte and enhanced effector CD8$^+$ T cell populations in CPI-Hep. Immunohistochemistry demonstrated co-localisation of CD8$^+$/granzyme B$^+$ T cells with CD68$^+$CCR2$^+$/CD68$^+$CD163$^+$ macrophages in CPI-Hep liver tissue.

Conclusions: CPI-Hep is associated with activation of peripheral monocytes and an enhanced cytotoxic, effector CD8$^+$ T cell phenotype. These changes were reflected by liver inflammation composed of CD163$^+$/CCR2$^+$ macrophages and CD8$^+$ T cells.

Lay summary: Some patients who receive immunotherapy for cancer develop liver inflammation, which requires cessation of cancer treatment. Herein, we describe ways in which the white blood cells of patients who develop liver inflammation differ from those of patients who receive the same immunotherapy but do not experience liver-related side effects. Targeting some of the pathways we identify may help to prevent or manage this side effect and facilitate cancer treatment.

Introduction

Cancer treatment has been revolutionised in the last decade by the emergence and widening use of a new class of immunotherapy; immune checkpoint inhibitors (CPIs). These cancer drugs are monoclonal antibodies targeting negative regulators of the immune system such as cytotoxic T-lymphocyte antigen-4 (CTLA-4), programmed cell death-1 (PD-1) and its ligand, programmed cell death ligand-1 (PD-L1).[1] Immune checkpoints play an important homeostatic role, preventing the generation of autoreactivity and immune-mediated tissue damage.[2]

Anti-CTLA-4 (ipilimumab), anti-PD-1 (*e.g.* nivolumab, pembrolizumab) and anti-PD-L1 (*e.g.* durvalumab, atezolizumab) treatments have been shown to be effective in various malignancies including melanoma, non-small-cell lung cancer and renal cell carcinoma and transformatively offer the possibility of durable remission even in the context of metastatic disease.[3–10] However, blocking these pivotal regulatory pathways has been associated with the emergence of a new class of drug side effect; immune-related adverse events (irAEs).[2] irAEs are autoimmune-like phenomena characterised by inflammation and immune-mediated tissue injury that may affect multiple organs, with CPI-related hepatitis (CPI-Hep) being among the most common.[2,11,12] Combination CPI therapy has been associated with an increased incidence of CPI-Hep and can affect up to 30% of patients on dual CPI treatment, 15% of whom develop severe hepatitis.[13,14] CPI-Hep presents a critical challenge in the application of immunotherapy with significant implications for quality of life and survivorship, given durable responses and also adjuvant therapy. This challenge is particularly important with the recent approval of CPI therapy for hepatocellular carcinoma (HCC), as the development of liver inflammation following CPI treatment may cause decompensation of a predisposed liver.[15] Thus, there is an urgent need to better understand the immunopathogenesis of this condition to allow for the development of rational

Keywords: immunotherapy; immunotherapy-related hepatitis; immune checkpoint.
Received 8 April 2020; received in revised form 25 January 2021; accepted 9 February 2021; available online 22 February 2021

* Corresponding author. Address: Liver Unit, QEQM Building, St Mary's Hospital, London, W2 1NY, UK; Tel.: +44 (0)203 312 1804, Fax: +44 (0)207 724 9369.
E-mail address: l.possamai@imperial.ac.uk (L.A. Possamai).
† Shared senior authorship.

https://doi.org/10.1016/j.jhep.2021.02.008

treatment strategies, which both protect the liver and preserve the anti-tumour efficacy of CPIs.

In this study, we aim to identify the immunological changes that occur with immune checkpoint inhibition in patients who develop CPI-Hep with dual or single agent CPI treatment. Herein, we characterise the phenotypic, functional and transcriptional profile of circulating and liver tissue-infiltrating myeloid and lymphoid subsets in patients with CPI-Hep and provide evidence for a CCR2^{high}CCR7^{low}CD163^{high}monocyte and HLA-DR^{high}I-COS^{high}Tim-3^{high}CD8-mediated pathogenesis in CPI-Hep.

Patients and methods

Patient characteristics

All patients were recruited between November 2017 and September 2019 from 3 centres (Charing Cross Hospital, The Royal Marsden Hospital and St. Mary's Hospital, London). Recruited CPI-treated patients were categorised into those who developed CPI-related hepatitis (CPI-Hep; n = 22) and those who did not develop hepatic irAE (CPI-noHep; n = 7) (Table 1). Healthy donors (HCs; n = 19) served as a control

Table 1. Clinical parameters of CPI-treated cancer patients with hepatitis compared to patients without hepatitis and healthy controls.

Parameters	CPI-Hep	CPI-noHep	Healthy controls
Number of patients	22	7	19
Age, year	61.0 [21.0–82.0]	73.0 [53.0–82.0]	32.0*** [21.0–65.0]
Gender (F:M)	5:17	4:3	8:11
Primary malignancy			n.a.
Melanoma	16	7	
Lung cancer	3		
Renal cell carcinoma	1		
Melanocytoma	1		
Tonsillar squamous cell cancer	1		
Immunotherapy			n.a.
Ipilimumab + nivolumab	14	1	
Pembrolizumab	3	5	
Nivolumab	1	1	
Durvalumab	1		
Atezolizumab	1		
anti-PD-1 adjuvant therapy	2		
Metastatic cancer *vs.* Adjuvant therapy			n.a.
Metastatic cancer	20	5	
Adjuvant	2		
Grade of hepatitis		n.a.	n.a.
Grade 2	9		
Grade 3	11		
Grade 4	2		
Peak ALT (IU/L)	261.0**** [121.0–1628.0]	20.50 [14.0–30.0]	n.a.
ALT (IU/L) 1 month follow-up	49.50#### [19.0–287.0]	23.0 [21.0–38.0]	n.a.
ALT (IU/L) 3 month follow-up	30.50#### [20.5–76.0]	24.0 [18.0–50.0]	n.a.
Fibroscan CAP (dB/m)	241.0 [166.0–308.0]	n.a.	n.a.
Fibroscan LSM (KPa)	6.650 [3.30–10.40]	n.a.	n.a.
Bilirubin (mmol/L)	10.50 [4.0–47.0]	11.50 [5.0–19.0]	n.a.
ALP	78.0 [41.0–1133.0]	76.0 [53.0–101.0]	n.a.
Monocytes (×10^9/L)	0.4 [0.2–2.0]	0.6 [0.5–7.7]	n.a.
Lymphocyte (×10^9/L)	1.1 [0.3–4.6]	1.1 [1.0–1.9]	n.a.
INR	1.00 [0.9–1.1]	n.a.	n.a.
Other irAE			n.a.
Aseptic meningitis	1		
Dermatitis	7		
Pneumonitis	4		
Cardiac	2		
Pancreatic	1		
Neurological	1		
Hypothyroidism	1		
Hypoadrenal	1		
None		5	
Patient outcome			n.a.
Complete response	6	2	
No recurrence	2		
Partial response	2		
Stable disease	1		
Progressive disease	8		
Not known	3	5	

ALP, alkaline phosphatase; ALT, alanine transaminase; CAP, controlled attenuation parameter; CPI-Hep, CPI-treated cancer patients with hepatitis; CPI-noHep, CPI-treated cancer patients without hepatitis; INR, international normalised ratio; irAE, immune-related adverse event; LSM, liver stiffness measurement. Data presented as median with minimum and maximum values. ***p = 0.0003; ****p <0.0001, compared with CPI-noHep, by one-way ANOVA; ####p <0.0001, compared with CPI-Hep peak ALT, by Mann-Whitney U test.

group. Sequential samples were taken from CPI-Hep patients at 1 month (n = 13) and 3 months (n = 7) following the first hepatology consultation. The study was approved by the Imperial College Tissue Bank (Ref. 12/WA/0196/R18009), City and East ethics committee (LREC 15/LO/0363), PEACE-(TRAcking Cancer Evolution through treatment (Rx), REC reference number 11/LO/0003) and TRACERx melanoma-(TRAcking Cancer Evolution through treatment (Rx), REC reference number 11/LO/0003).

Flow cytometry and absolute cell counts

Surface and intercellular staining of isolated peripheral blood mononuclear cells (PBMCs) were carried out using fluorochrome-labelled monoclonal antibodies (Table S1). The acquisition was performed on the LSR Fortessa™ flow cytometer and data were acquired using the BD FACSDiva™ software (Becton Dickinson Ltd, Oxford, UK). Data was analysed with the FlowJo software 10.6.0.

Serum levels of soluble CD163 (sCD163)

sCD163 was assessed in human sera using enzyme-linked immunosorbent assay (ELISA) (R&D Systems, Abingdon, UK). The optical density was measured at 450 nm using the Multiskan Go plate reader (Thermo Fisher Scientific, Hemel Hempstead, UK).

Phagocytosis assays and oxidative burst

Phagocytosis of *Escherichia coli* (*E. coli*) was evaluated in monocytes using the pHrodo™ Green *E. coli* BioParticles™ (ThermoFisher Scientific, Hemel Hempstead, UK) and monocyte oxidative burst was assessed using the Burstest™ (Phagoburst™) kit (Becton Dickinson Ltd, Oxford, UK), according to the manufacturer's instructions.

In vitro monocyte-derived macrophage differentiation and functional assessment

Isolated $CD14^+$ monocytes from HCs and CPI-Hep patients (n = 3/group) were spontaneously differentiated into monocyte-derived macrophages (MoMFs) *in vitro* for up to 48 hours. In the last 5 hours of the culture, cells were stimulated with 100 ng/ml of lipopolysaccharide (LPS). Cells were harvested and assessed by flow cytometry and supernatants were analysed using Meso Scale Discovery (MSD) system (Rockville, USA).

Nanostring gene expression profiling

Gene expression analysis of the transcriptional profile of monocytes and $CD8^+$ T cells from HCs, CPI-Hep and CPI-noHep (n = 4/group) was performed using the NanoString nCounter® GX Human Immunology V2 assay (NanoString™ Technologies, Seattle, Washington, USA) following manufacturer's instructions.

Immunohistochemistry and immunofluorescence

Liver biopsy tissue was obtained from CPI-Hep patients (n = 4) and pathological controls [hepatic resection margins of colorectal metastases, (n = 2)]. Post-mortem samples were obtained from CPI-noHep patients (n = 3).

For further details regarding the materials used, please refer to the CTAT table and supplementary information.

Results

Patient characteristics

In this study, 22 cancer patients with CPI-Hep were recruited and compared to 7 CPI-noHep patients and 19 HCs (Table 1). The median age of the CPI-Hep cohort was 61 years old, 77% were male. Although patients treated with CPIs were significantly older than HCs, there were weak or no significant correlations of markers of interest with age (Fig. S1 & Table S6).

Melanoma was the primary malignancy in most patients, of whom most received combination immunotherapy, ipilimumab+nivolumab (14/22), for metastatic disease (20/22). Patients with CPI-Hep (grade 2-4 hepatitis) presented with a significantly elevated median alanine transaminase (ALT) compared to CPI-noHep patients (261.0 *vs.* 20.50 IU/L, respectively; p <0.0001), which decreased significantly in 1-month and 3-month follow-up blood tests (261.0 *vs.* 46.0 and 30.0 IU/L, respectively; p <0.0001). Other parameters such as bilirubin, alkaline phosphatase (ALP) levels, circulating monocyte and lymphocyte counts and international normalised ratio (INR) were not altered in CPI-Hep compared to CPI-noHep patients. Notably, 16/22 patients with CPI-Hep developed other irAEs. The response of patients with CPI-Hep to immunotherapy was heterogeneous, with patients showing a complete response (6/22), no recurrence or partial response (2/22, respectively), stable disease (1/22) and progressive disease (8/22) (Table 1 & Table S7).

Marked reduction in total peripheral monocyte counts coupled with an increased frequency of $CD14^{++}CD16^-$ classical subset in patients with CPI-Hep

Monocyte recruitment to the liver from peripheral blood has been shown to be important in the pathogenesis of other acute liver injury syndromes.[16–19] We assessed absolute numbers and proportions of monocyte subsets in HCs, and patients with CPI-Hep and CPI-noHep using flow cytometry. We distinguished between non-classical $CD14^+CD16^{++}$, intermediate $CD14^{++}CD16^+$ and classical $CD14^{++}CD16^-$ (Fig. 1A & Fig. S2A). Patients with CPI-Hep showed a significant reduction of the absolute numbers of total $CD14^+$ monocytes compared to HCs (p = 0.04) but not CPI-noHep (Fig. 1A). This reduction was further reflected in the classical monocyte compartment of patients with CPI-Hep (p = 0.0003) (Fig. 1A). Patients with CPI-Hep presented the lowest proportion of non-classical monocytes, compared to HCs and CPI-noHep (4.179% ±1.043% *vs.* 7.916% ±0.9632% and 13.80% ±2.417%, respectively) and the highest proportion of classical monocytes (93.80% ±1.394% *vs.* 87.92% ±1.127% and 82.61% ±2.559%, respectively) (Fig. 1A). The frequency of non-classical monocytes in patients with CPI-Hep correlated negatively with ALT levels (r = −0.51; p = 0.02), whereas the frequency of classical monocytes correlated positively with ALT (r = 0.52; p = 0.02) (Fig. S2B).

Patients with CPI-Hep display increased levels of soluble and cell surface expression of CD163

sCD163/CD163 were shown to be a marker of monocyte/macrophage activation.[20–23] Circulating monocytes in CPI-Hep patients had increased CD163 mean fluorescence intensity (MFI) levels (Fig. 1B & Fig. S2A). This was particularly noted in the intermediate monocyte subset when compared to HCs and CPI-noHep patients (2,892 ±457.8 *vs.* 686.3 ±28.65 and 958.1 ±190.5, respectively), whilst significant upregulation of CD163 expression on classical monocytes was only significant when

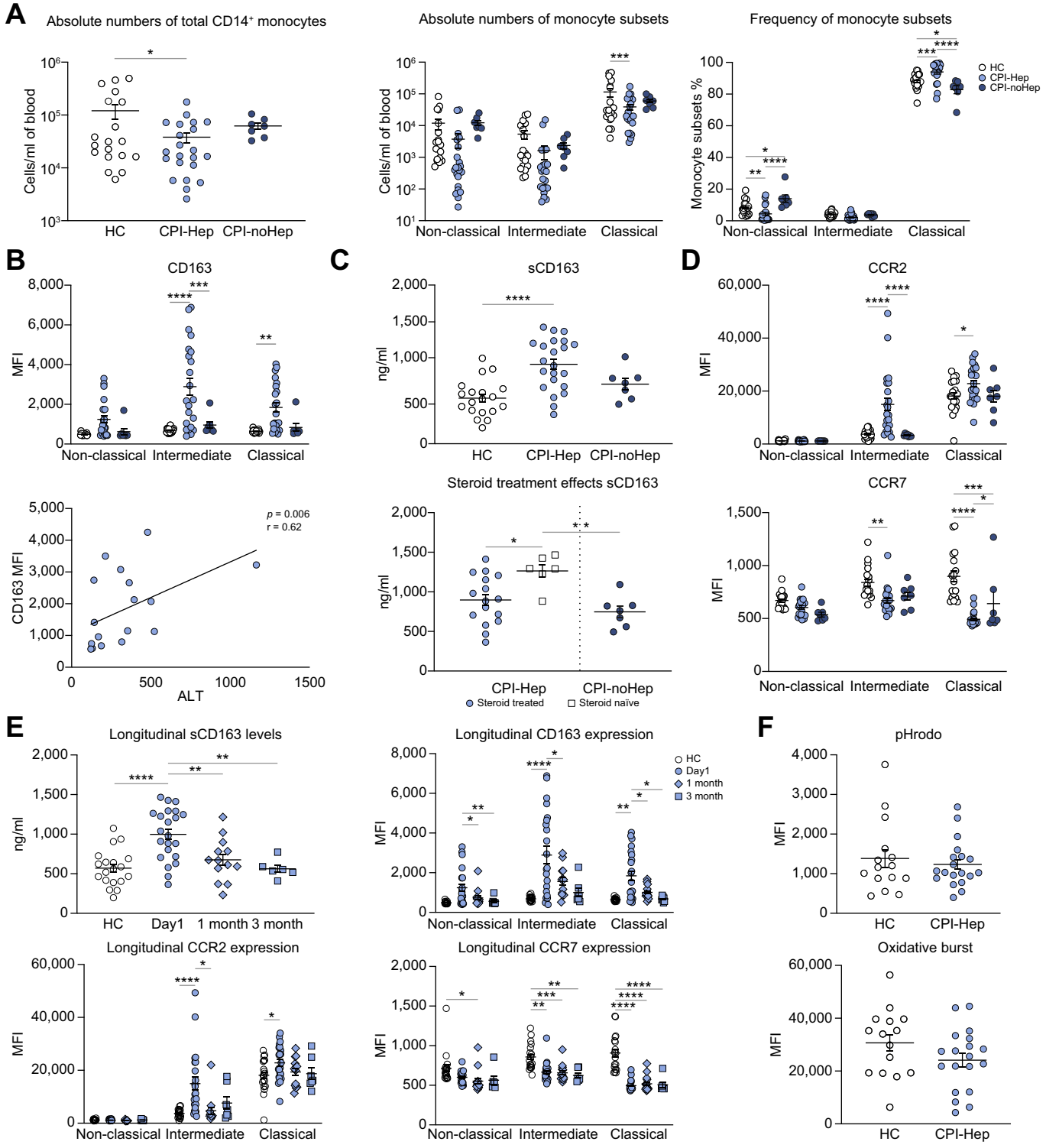

Fig. 1. Serum sCD163 levels, phenotypic and functional characterisation of circulating monocytes. ELISA and flow cytometry analysis of circulating monocytes of HCs (n = 19), CPI-Hep (n = 22) and CPI-noHep (n = 7). (A) Absolute numbers and frequency of circulating monocyte subsets (one-way ANOVA). (B) MFI expression levels of the activation marker CD163 in monocyte subsets (one-way ANOVA). Spearman correlation of CD163 (MFI) expression on total CD14$^+$ monocytes with ALT levels in CPI-Hep. (C) Levels of sCD163 in serum of HC, CPI-Hep and CPI-noHep (Kruskal-Wallis). Comparison of sCD163 in steroid-treated (n = 16) and steroid-naïve (n = 6) CPI-Hep patients to CPI-noHep (Mann-Whitney *U* test). (D) MFI expression of chemokine receptors (CCR2, CCR7) (one-way ANOVA). (E) Longitudinal analysis of sCD163 in serum CPI-Hep at 1 month follow-up (n = 13) and 3-month follow-up (n = 6) samples, compared to HC and CPI-Hep (Wilcoxon matched-pairs test). Longitudinal flow cytometry analysis of monocyte phenotype including activation and chemokine receptors from CPI-Hep at 1 month (n = 13) and 3 month follow-up (n = 7) samples, compared to HC and CPI-Hep (Wilcoxon matched-pairs test). (F) MFI of *E. coli* uptake (pHrodo) and ROS production (oxidative burst) gated on total CD14$^+$ monocytes in whole blood of HC (n = 15) and CPI-Hep (n = 19) (Mann-Whitney *U* test). $^*p$ <0.05, $^{**}p$ <0.01, $^{***}p$ <0.001, $^{****}p$ <0.0001. ALT, alanine aminotransferase; HCs, healthy controls; MFI, mean fluorescence intensity; ROS, reactive oxygen species.

compared to HCs (p = 0.0015) (Fig. 1B). This cell surface increase in CD163 expression correlated positively with ALT levels in CPI-Hep (r = 0.62; p = 0.006) (Fig. 1B). Elevated sera levels of sCD163 were also detected in CPI-Hep patients compared to HCs (p <0.0001) (Fig. 1C). When compared to CPI-noHep patients, differences did not reach statistical significance. However, when stratified based on administration of immunosuppressive steroids, sCD163 levels were significantly elevated in non-steroid-treated CPI-Hep patients compared to both CPI-noHep (p = 0.002) and CPI-Hep steroid-treated patients (p = 0.01) (Fig. 1C). None of the changes reported in the activation profile on monocytes and in the circulation of CPI-Hep patients were affected by differences in CPI treatment regimen (Fig. S3A).

Peripheral monocytes in CPI-Hep are characterised by a CCR2^{high}CCR7^{low} tissue homing phenotype

Next, to understand the role of the reported monocytic phenotype in the pathogenesis of CPI-Hep, we explored their migratory capacity to the inflamed liver tissue. Chemokine receptor profiling revealed that intermediate monocytes from CPI-Hep patients expressed increased levels of the tissue homing receptor CCR2 when compared to HCs and CPI-noHep (14,976 ±2,585 *vs.* 3,742 ±373.6 and 3,281 ±179.5, respectively). The highest levels however were detected in the classical population and were significantly elevated in CPI-Hep patients compared to HCs (p = 0.04) (Fig. 1D). In contrast, the expression of the lymph node homing receptor CCR7 was significantly reduced in the CPI-Hep patients intermediate (p = 0.009 compared to HC) and classical (p <0.0001 and p = 0.4 compared to HC and CPI-noHep, respectively) monocyte subsets (Fig. 1D). The effect of combination therapy was not distinct to that of single therapy regimen in inducing a CCR2^{high}CCR7^{low} phenotype in CPI-Hep patients (Fig. S3A).

Discontinuation of CPI therapy with use of corticosteroids reverses the main phenotypic alterations observed in monocytes from CPI-Hep patients

Monocyte phenotype was further evaluated longitudinally in CPI-Hep patients following withdrawal of CPI therapy, treatment with immunosuppressants and improvement in liver inflammation. Of the cell surface markers tested, no significant differences were detected in the immunophenotype based on steroid

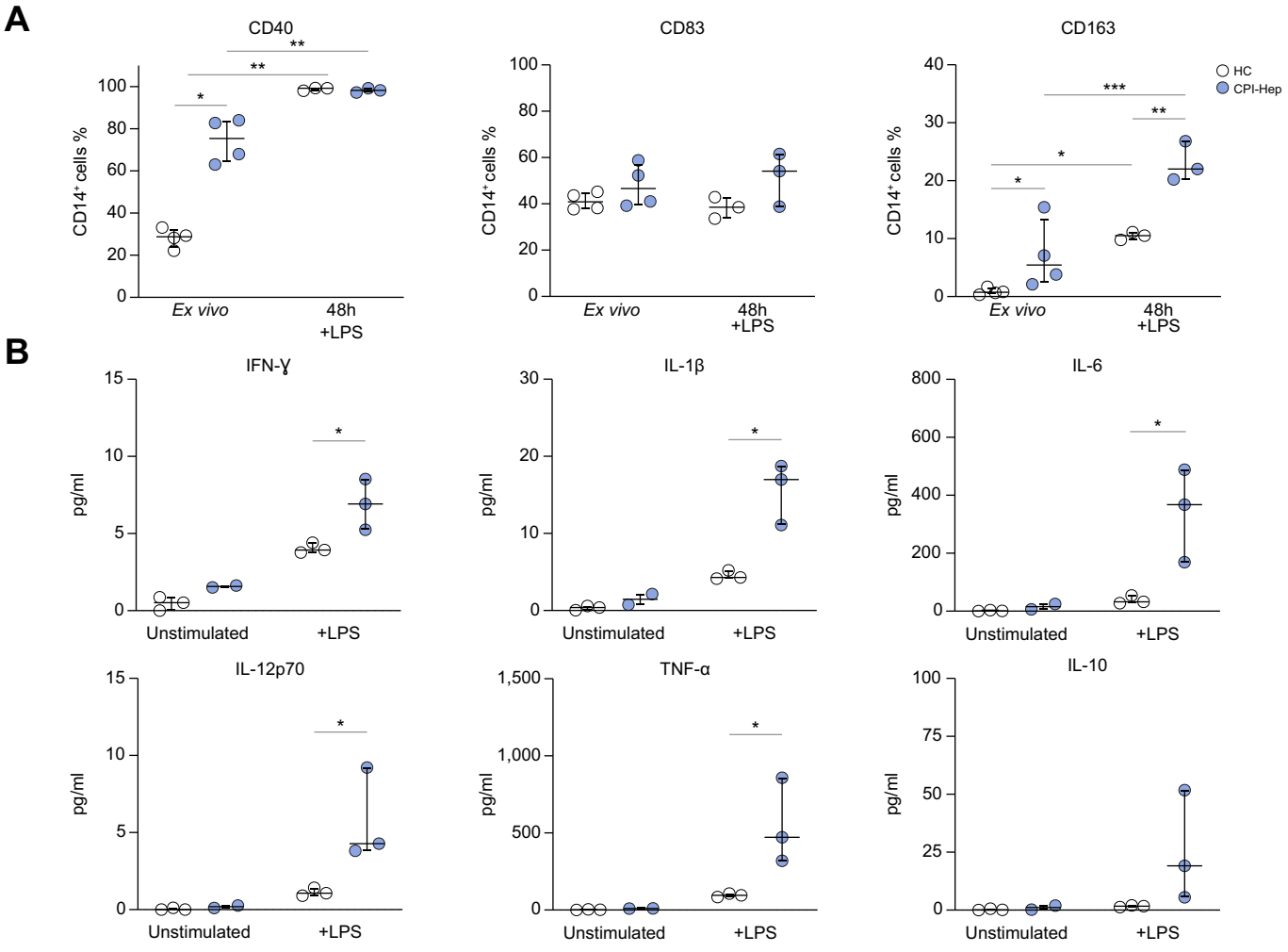

Fig. 2. *In vitro* differentiated MoMFs from patients with CPI-Hep show inflammatory function. (A) Data show surface marker expression in monocytes *ex vivo* and in MoMFs after 48 hours of culture. 100 ng/ml of LPS was added to the cells in the last 5 hours of culture (Mann-Whitney *U* test). (B) Levels of inflammatory cytokines secreted by MoMFs after 24 hours of culture following LPS-stimulation (Mann-Whitney *U* test). *p <0.05, **p <0.01, ***p <0.001. LPS, lipopolysaccharide; MoMFs, monocyte-derived macrophages.

treatment of samples collected at enrolment (day 1) (Fig. S4A). However, when compared to day 1 samples, cell surface expression, as well as soluble levels of CD163, were reduced at both 1- and 3-month follow-ups, approaching levels seen in HCs (Fig. 1E). Similarly, the elevated CCR2 expression was diminished in sequential samples (Fig. 1E). An opposite trend was observed in CCR7 expression, which remained persistently reduced throughout the course of follow-up (Fig. 1E).

Circulating monocytes from CPI-Hep maintain their functional ability for effective microbial clearance

Functional defects in monocyte phagocytosis and/or oxidative burst are well recognised in acute liver failure (ALF) and alcoholic hepatitis.[24–26] We hypothesised this may also be the case in CPI-Hep. Circulating monocytes from CPI-Hep demonstrated an unaltered microbial clearance capacity coupled with high production of reactive oxygen species (ROS) as measured by the oxidative burst assay compared with HCs (Fig. 1F & Fig. S2C).

In vitro spontaneously differentiated monocyte-derived macrophages from patients with CPI-Hep show pro-inflammatory properties

As we have established an inflammatory $CD163^{high}CCR2^{high}$ tissue-homing phenotype of peripheral monocytes in patients with CPI-Hep, we aimed to address the functionality of those monocytes once differentiated into macrophages, in order to mimic liver MoMFs in CPI-Hep. To this end, the *ex vivo* activation profile of monocytes from HCs and CPI-Hep patients was compared to *in vitro* spontaneously differentiated MoMF. Subsequently, we assessed the secretion of inflammatory cytokines by MoMF from CPI-Hep patients compared to HCs. Phenotyping revealed an increased frequency of $CD14^+$ monocytes expressing the activation markers CD40 and CD163 *ex vivo*, while the proportion of CD83-expressing monocytes remained similar to HCs (Fig. 2A). Following stimulation with LPS, MoMFs from both, HCs and CPI-Hep patients showed an increased frequency of CD40 and CD163 expression (Fig. 2A). However, the frequency of $CD163^+CD14^+$ monocytes was significantly higher in CPI-Hep patients compared to HC. Levels of inflammatory cytokines (IFNγ, IL-1β, IL-6, IL-12p70, TNFα) secreted by MoMFs from CPI-Hep patients following LPS-stimulation were significantly increased compared to HC levels (Fig. 2B), while no differences were detected in IL-10 levels.

Increased gene expression of activation and reduction of negative regulators are characteristics of peripheral monocytes in CPI-Hep

Gene expression profiling of flow-sorted monocytes (Fig. S5A) from representative HC, CPI-Hep and CPI-noHep patients was carried out using quantitative NanoString™ gene expression arrays. Compared to CPI-noHep, monocytes from patients with CPI-Hep showed a significantly increased expression of survival factors (*FLT3, PF4*), macrophage activation and polarisation (*CD163, GATA3, JUN*) and the complement factor *C1QB*. In contrast, transcription factors (*NRIP3, NR4A1*), cytokines (*TNFSF9, IL1B*) and immune regulatory molecules (*DUSP2,* GADD45B, *CD83, PTGS2, GPR183*) were significantly reduced in monocytes from patients with CPI-Hep (Fig. 3A&B; Fig. S5B). The monocytic distinct transcriptional profile between CPI-Hep and CPI-noHep patients was explored further between CPI-Hep and HCs, confirming upregulation of the macrophage activation marker *CD163* and identifying upregulation of survival factors (*PF4, FLT3*) (Fig. 3A).

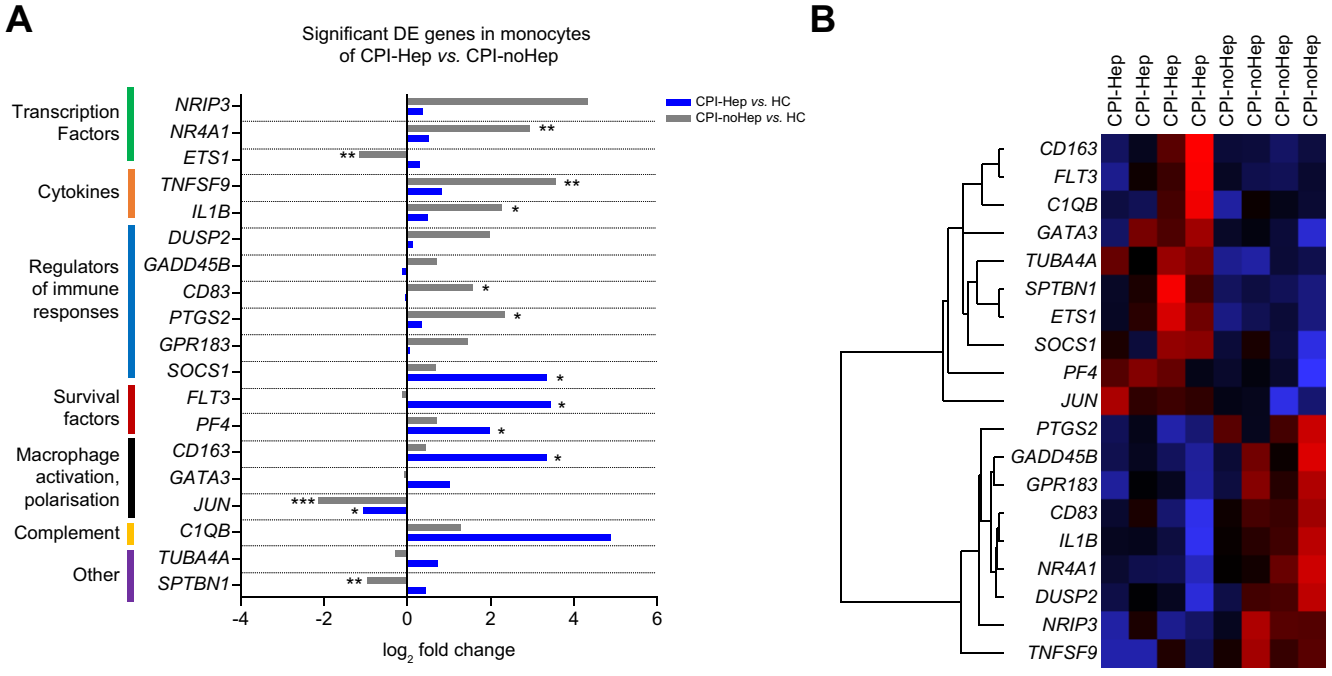

Fig. 3. Gene expression pattern of peripheral monocytes. Quantitative microarray gene expression analysis of HCs (n = 4), CPI-Hep (n = 4) and CPI-noHep (n = 4) using NanoString Technologies. (A) Data show log2-fold change of significantly DE genes and (B) agglomerative cluster (heatmap, z-score; blue = min and red = max magnitude of expression) of monocytes in CPI-Hep *vs.* CPI-noHep. For every such gene expression, CPI-Hep (blue bars) and CPI-noHep (grey bars) were compared to baseline of HCs. **p* <0.05, ***p* <0.01, ****p* <0.001 (Wald test). DE, differentially expressed; HCs, healthy controls.

Peripheral CD8$^+$ T cells in CPI-Hep are predominantly HLA-DR^{high}ICOS^{high}Tim3^{high}

Next, we characterised circulating T cells in CPI-Hep patients, compared to HCs and CPI-noHep patients (Fig. S6A). Proportions, as well as absolute numbers of CD8$^+$, CD4$^+$ and regulatory T cells (Tregs) were comparable between HCs, CPI-Hep and CPI-noHep patients (Fig. S6B). Flow cytometry analysis showed no differences in CD4$^+$ T cell activation status or Treg proportions compared to CPI-noHep patients, though some treatment-related changes were observed (Fig. S6C). As CD8$^+$ T cells were implicated to be important mediators of immune-mediated liver damage,[27–29] detailed immunophenotyping of CD8$^+$ T cells was performed. CD8$^+$ T cells in CPI-Hep patients showed an increased frequency of expression of the activation markers ICOS and HLA-DR (ICOS: 9.128% ±1.414% *vs.* 2.397% ±0.5977% and 3.477% ±0.5378%; HLA-DR: 19.98% ±3.087% *vs.* 4.200% ±0.5881% and 6.397% ±0.7769% in CPI-Hep, HCs and CPI-noHep, respectively) (Fig. 4A). Notably, the frequency of activated ICOS^{high}CD8$^+$ T cells correlated positively with sCD163 levels (r = 0.61, p = 0.004) (Fig. S6D). This was accompanied by a significant increase in the frequency of CD8$^+$ T cells expressing the inhibitory markers Tim3 in CPI-Hep patients compared to both controls (p = 0.0009 and p = 0.02) and Lag3 compared to HCs (p = 0.04) (Fig. 4B). This significant increase in the frequency of CD8$^+$ T cells expressing markers of activation in CPI-Hep patients remained elevated following treatment with corticosteroids and continued to be elevated after up to 1 month of follow-up (Fig. S4B, Fig. 4A&B). Evaluation of differences in CPI treatment regimen on the CD8$^+$ T cell phenotype in CPI-Hep showed no distinct effects on markers associated with activation (Fig. S3B).

Increased cytotoxicity in peripheral CD8$^+$ T cells from CPI-Hep

We examined the production of the cytolytic mediators granzyme B and perforin. Intracellular cytokine staining revealed an increased frequency of CD8$^+$ T cells producing granzyme B in CPI-Hep patients compared to HC and CPI-noHep patients (54.56% ±4.616% *vs.* 19.79% ±4.212% and 25.03% ±5.905%, respectively). Significantly enhanced levels of perforin were detected in CD8$^+$ T cells in CPI-Hep patients compared to HCs and CPI-noHep patients (48.87% ±3.486% *vs.* 27.56% ±4.196% and 25.22% ±5.564%, respectively) (Fig. 4C). Similar to the activation markers, the frequency of CD8$^+$ T cells producing cytolytic mediators remained elevated over the first month of follow-up and steroid treatment (Fig. 4C, Fig. S4B). Functional markers were not affected significantly by differences in CPI treatments (Fig. S3B).

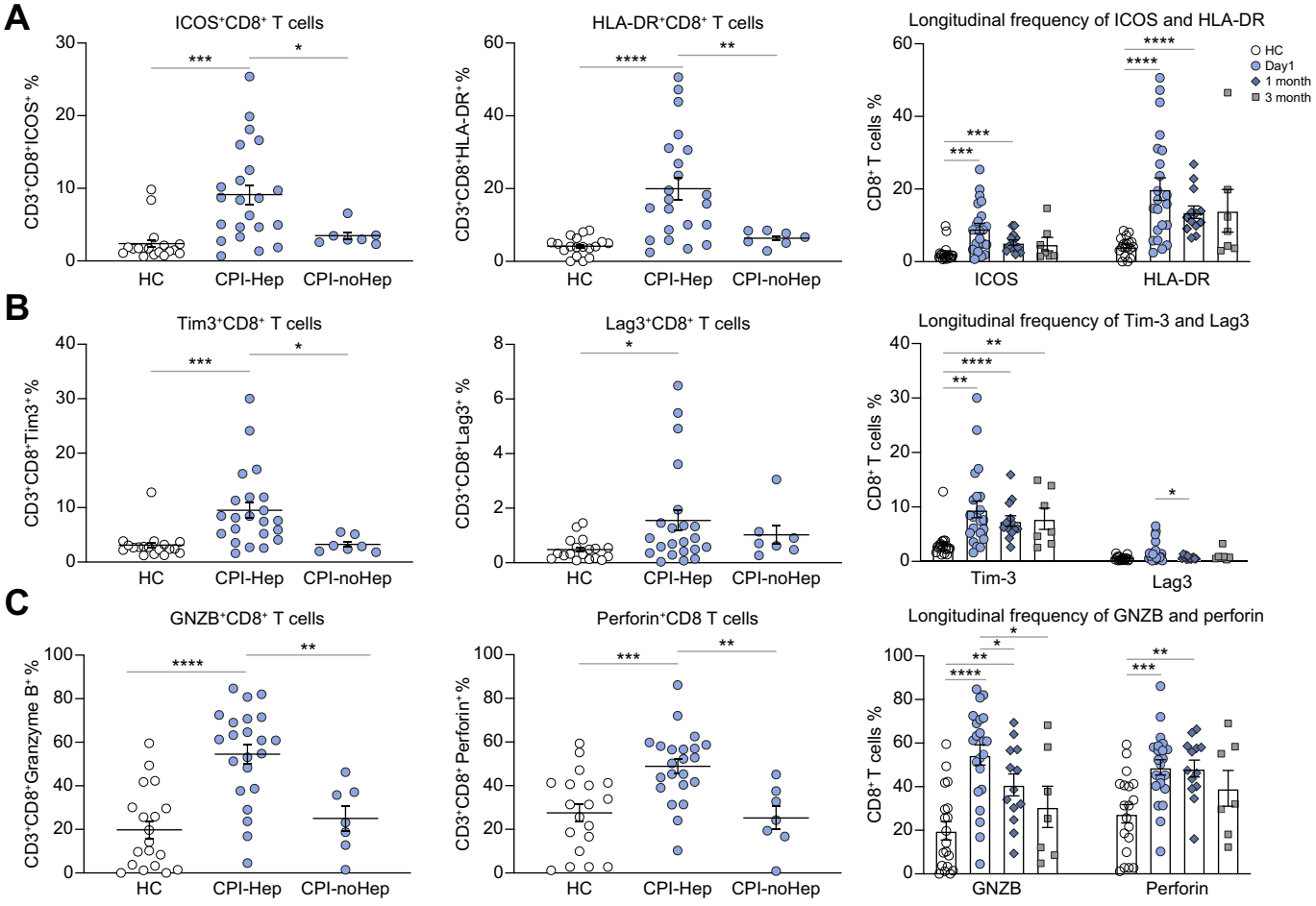

Fig. 4. Phenotypic characterisation of circulating T cell populations. Flow cytometry analysis of circulating T cells of HCs (n = 19), CPI-Hep (n = 22) and CPI-noHep (n = 7) (Kruskal-Wallis). Longitudinal analysis of CD8$^+$ T cells from CPI-Hep at 1 month follow-up (n = 13) and 3-month follow-up (n = 7) samples (Wilcoxon matched-pairs test). (A) Frequency of CD8$^+$ T cells expressing markers for activation (ICOS, HLA-DR) and (B) inhibitory markers (Tim-3, Lag-3) in CPI-Hep. (C) Frequency of intracellular granzyme B and perforin in CD8$^+$ T cells. *p <0.05, **p <0.01, ***p <0.001, ****p <0.0001. HCs, healthy controls.

Activated CD8$^+$ T phenotype in CPI-Hep patients is confirmed by transcriptional profiling

Subsequently, the gene signature of flow-sorted CD8$^+$ T cells (Fig. S5A) from CPI-Hep patients was also determined using NanoString^{TM} gene expression array. CD8$^+$ T cells from patients with CPI-Hep compared to CPI-noHep had an upregulated T cell activation and costimulatory gene profile (*CD6, NFKB1, IMPDH2, CD27*); T cell development, differentiation and functional markers (*CD45RA, DNMT3A*), both associated with naïve/effector T cells; T cell trafficking (*SELL, CCR7*), cytokine signalling (*ISG20, IL6ST, IL6R*) and immune checkpoints (*HAVCR2, CTLA4*). Downregulated genes included genes associated with cytotoxicity and regulation of cytotoxicity (*GZMA, GNLY, SLAMF7*), T cell development, differentiation and functional markers (*PTPN22, ITGAL, PSTPIP1, EOMES, WNT10B, CD45RO*), associated with memory T cells; and negative regulators (*SMAD3, CD59, RORA, TIGIT, HLA-C, LILRB1*) (Fig. 5A&B; Fig. S5C). Compared to HCs, CPI-Hep showed upregulation of the immune checkpoints (*HAVCR2* and *CTLA4*) and T cell activation/cytokine signalling (*PLCG2, ISG20*) (Fig. 5A).

Intrahepatic CD68$^+$CCR2$^+$/ CD163$^+$ and CD8$^+$ inflammatory immune aggregates are enriched in livers of CPI-Hep patients

In view of the reported phenotypic and transcriptional changes of circulating monocytes and CD8$^+$ T cells in CPI-Hep patients and the activated pro-inflammatory functional profile of *in vitro* MoMFs, we next investigated immune cell recruitment/enrichment of these populations within liver tissue using immunohistochemistry and immunofluorescence. To this end, liver biopsies from patients with CPI-Hep were stained and compared to pathological control tissue (hepatic resection margins of colorectal metastases) and post-mortem liver samples from CPI-noHep patients. Notably, the predominant CPI regimen in CPI-Hep and CPI-noHep was combination ipilimumab+nivolumab (Table S4). Patients with CPI-Hep showed lobular liver inflammation and focal aggregates of increased, but non-significant, numbers of intrahepatic CD163$^+$ and CD68$^+$ macrophages and CD3$^+$ and CD8$^+$ T cells (Fig. 6A–D), whereas pathological controls and post-mortem liver tissue of CPI-noHep patients show fewer and evenly distributed macrophages with

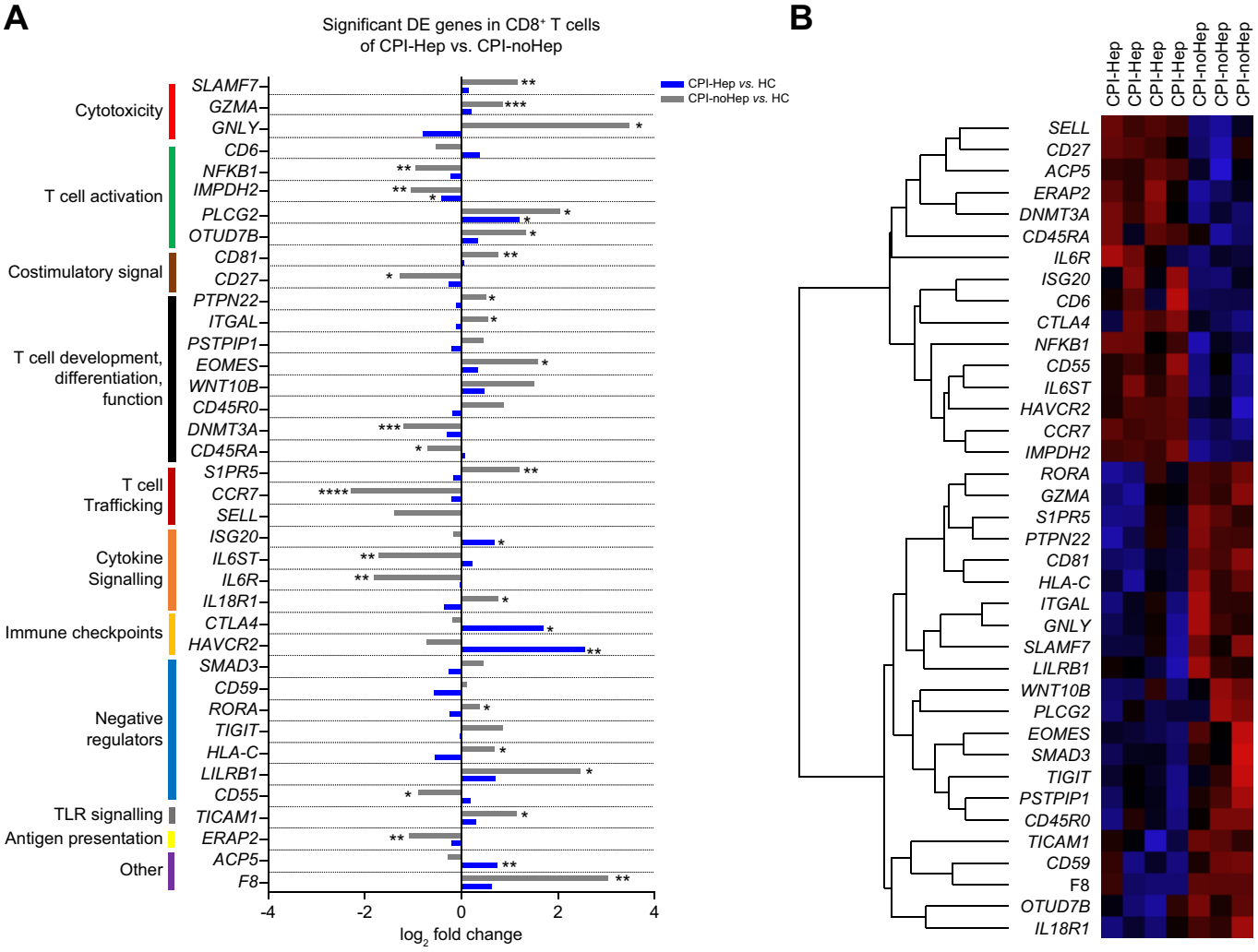

Fig. 5. Gene expression pattern of peripheral CD8$^+$ T cells. Quantitative microarray gene expression analysis of HCs (n = 4), CPI-Hep (n = 4) and CPI-noHep (n = 3) using NanoString Technologies. (A) Data show log2 fold change of significantly DE genes and (B) agglomerative cluster (heatmap, z-score; blue = min and red = max magnitude of expression) of CD8$^+$ T cells in CPI-Hep *vs.* CPI-noHep. For every such gene expression, CPI-Hep (blue bars) and CPI-noHep (grey bars) were compared to baseline of HC. *p <0.05, **p <0.01, ***p <0.001, ****p <0.0001 (Wald test). DE, differentially expressed; HCs, healthy controls.

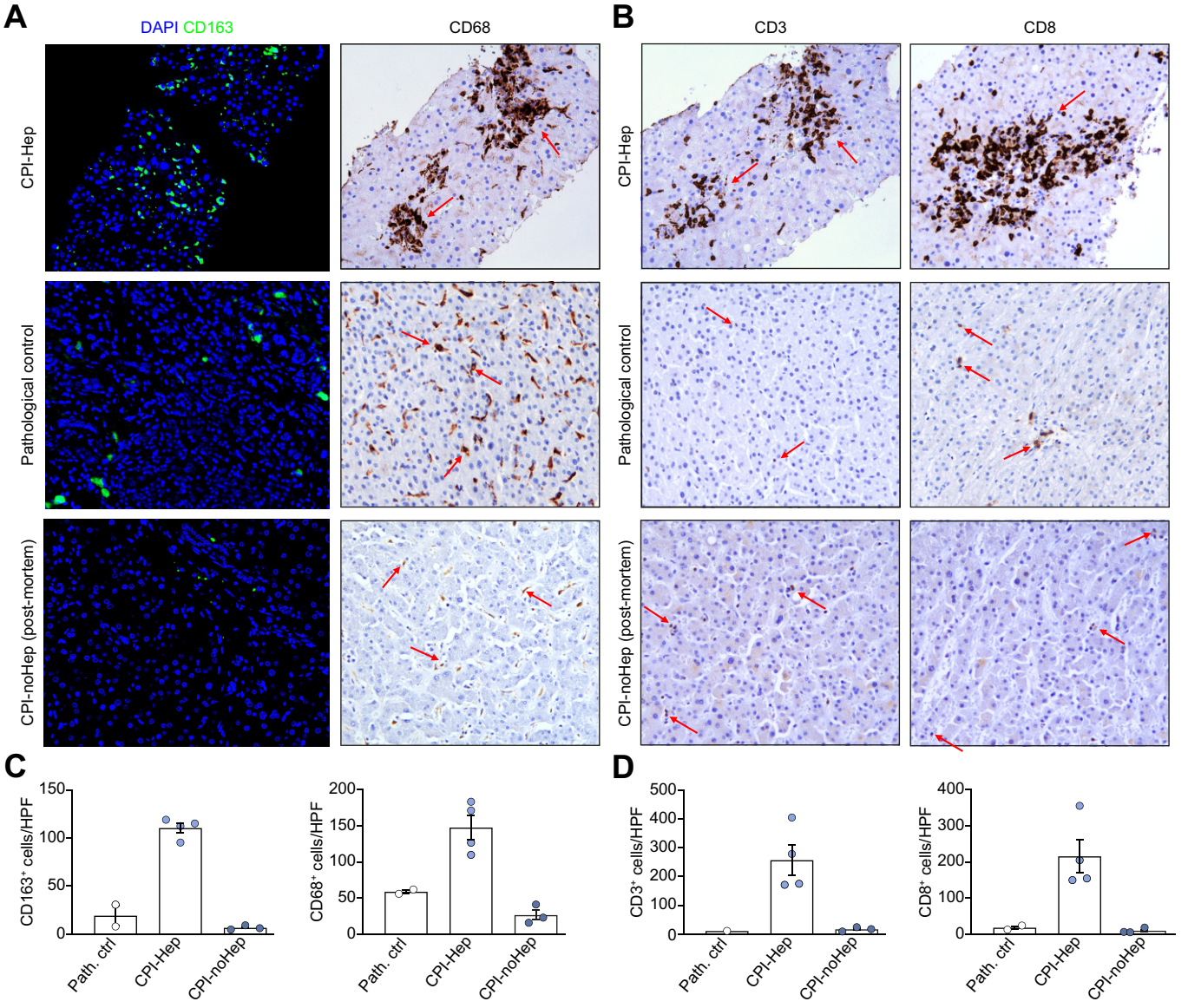

Fig. 6. Immune staining of intrahepatic macrophages and CD8⁺ T cells. Representative pictures of liver biopsies of CPI-Hep (n = 4), pathological control (n = 2) and post-mortem tissue from CPI-noHep (n = 3). (A) Single stains for CD163, CD68, (B) CD3 and CD8 with 200× magnification. (C) Absolute numbers of $CD163^+$, $CD68^+$ (Kruskal-Wallis) and (D) $CD3^+$ and $CD8^+$ cells per HPF (Kruskal-Wallis). HPF, high power field.

typical Kupffer cell morphology and $CD8^+$ T cells (Fig. 6A&B). Analyses further revealed the presence of CCR2 and granzyme B-positive cells within focal aggregates in liver tissue of patients with CPI-Hep (Fig. 7A&B). In addition, double immune stains revealed co-localisation of $CD68^+$ macrophages with $CD163^+$ and $CCR2^+$ expression and the close proximity of cytotoxic $CD8^+$ T cells with $CD68^+$ macrophages within immune aggregates in livers of patients with CPI-Hep (Fig. 7C–E).

Discussion

This work has provided the first characterisation of the peripheral and intrahepatic immune phenotype and transcriptional profile of human T cells and monocytes/macrophages in patients with CPI-Hep.

The presence of $CCR2^{high}CCR7^{low}$ classical monocytes in blood and the reduction of the absolute numbers of classical monocytes, combined with the increased presence of $CD68^+CCR2^+$ macrophages in liver biopsies, suggests monocyte recruitment to the liver from the circulating monocyte pool may be mechanistically important in the pathogenesis of CPI-Hep. In paracetamol and carbon tetrachloride-induced liver injury the CCR2-mediated recruitment of inflammatory classical monocytes has been shown to drive hepatocyte injury and fibrosis.[16,18,19] In human paracetamol-induced ALF a relative monocytopaenia is also observed with avid recruitment of monocytes to the liver, where evidence suggests they mature into MoMFs.[17]

Additional evidence of monocyte activation in CPI-Hep comes from our observation of upregulation of CD163 on both a transcriptional level and MFI expression of CD163 on the cell surface of monocytes, which correlated with disease severity; this was further reflected in the liver by co-localisation of intrahepatic CD163 with CD68. Moreover, *in vitro* differentiated MoMFs from

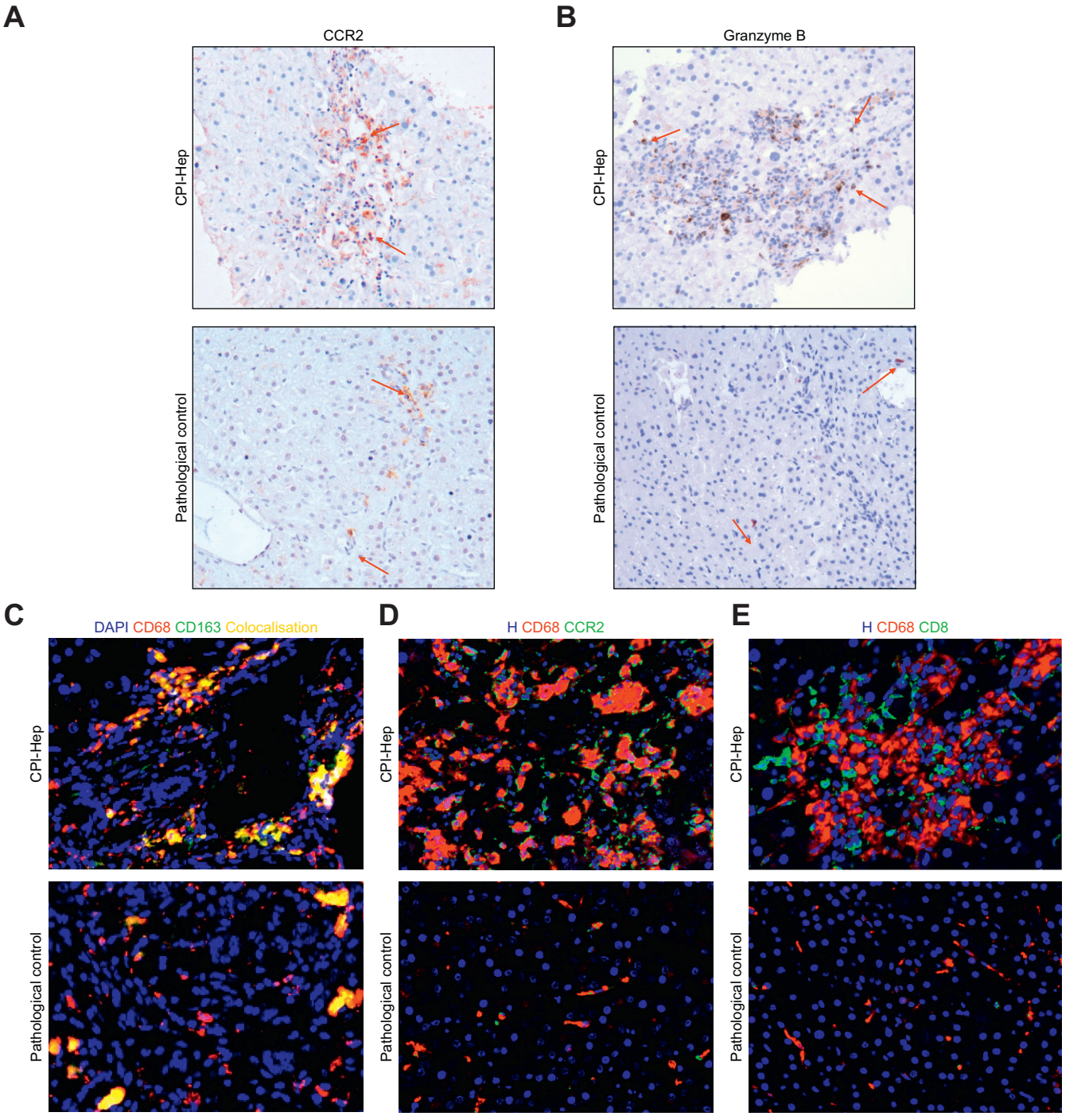

Fig. 7. Immune staining of intrahepatic CD163$^+$ and CCR2$^+$ macrophages and CD8$^+$ T cells. Representative pictures of liver biopsies of CPI-Hep (n = 4) and pathological control (n = 2). (A) Single stains for CCR2 and (B) Granzyme B with 200× magnification. (C) Double stains for CD68/CD163 (D) CD68/CCR2 and (E) CD68/CD8 with 400× magnification.

patients with CPI-Hep show an increased frequency of CD163 expression, suggesting that the peripheral activated phenotype is maintained on differentiation. Previous studies have provided substantial evidence that CD163 and sCD163 are biomarkers of monocyte/macrophage activation in liver disease.[21,22] Serum levels of sCD163 have previously been reported to be significantly raised in patients receiving CPIs who developed any organ irAE.[30] We replicated this finding, noting an increase in sCD163 in sera from our patient cohort with CPI-Hep, indicating that the CD163/sCD163 axis may have potential as a biomarker for irAE and CPI-Hep in particular.

Moreover, this activated monocyte/MoMF profile was accompanied by the increased production of pro-inflammatory cytokines by *in vitro* MoMFs from patients with CPI-Hep. This indicates an inflammatory 'M1-like' polarisation with enhanced pro-inflammatory capacity of MoMFs in the pathogenesis of CPI-

Hep. Evidence of monocyte activation is further enhanced by gene expression profiling in monocytes, which demonstrated downregulated expression of regulators of immune responses and T cell activation in CPI-Hep. These include GPR183, a negative regulator of Type I IFN responses and regulator of TLR-mediated responses,[31] as well as PTGS2, an enzyme which catalyses the generation of prostaglandins.

In addition to changes in monocyte phenotype and gene expression, we observed differences within the T cell compartment in CPI-Hep patients. Interestingly, the $CD4^+$ T cell population shows less phenotypic alteration associated with either CPI treatment or toxicity than the CD8 population. In our cohort, circulating $CD8^+$ T cells of CPI-treated patients show a distinct effector/effector memory phenotype, compared to HCs. We also provide evidence that, when compared to CPI-noHep, $CD8^+$ T cells in CPI-Hep patients present an effector-like transcriptional profile and dysregulated effector memory formation ($CD45RA^+CD45RO^-EOMES^{low}WNT10B^{low}DNMT3A^{high}$ transcriptional profile).[32]

Effector $CD8^+$ T cells, once activated, show strong T cell receptor, costimulatory and cytokine signalling. This is consistent with our observations of increased HLA-DR and ICOS expression at the protein level, and the upregulation of genes such as NFKB1, IL-6 receptors and ISG20.[33–36] In CPI-Hep, $CD8^+$ T cells further show an upregulation of genes associated with T cell responsiveness and cytolytic activity (CD6, IMPDH2)[37] and a downregulation of genes important for regulating immune responses in $CD8^+$ T cells (PTPN22, LILRB1, TIGIT, CD81, SLAMF7 and CD59), which regulate cytotoxicity to limit autoreactivity/autoimmunity.[38–41]

In accordance with our phenotypic observations in patients with CPI-Hep, effector $CD8^+$ T cells produce cytolytic mediators such as granzyme B and perforin in high levels.[42] In contrast, effector memory T cells, as seen in the CPI-noHep cohort, are granzyme A^+ but only express low levels of granzyme B and perforin with limited cytotoxic activity without prior stimulation.[42] Although, we observe a discordance of cytolytic mediators in gene/protein expression, the increased presence of granzyme B^+Perforin$^+CD8^+$ T cells in the periphery, coupled with CD8/granzyme B co-localisation in liver biopsies and the proven reduction of expression of regulating factors suggests CD8-mediated cytotoxicity may play an important role in the pathogenesis of hepatocyte injury in CPI-Hep. This is in line with recent studies showing that infiltration of activated $CD8^+$ T cells in other forms of drug-induced liver injury is associated with liver pathology.[27]

Finally, the co-localisation of CCR2/CD68 macrophages with cytotoxic T cells observed in liver biopsies raises questions about the nature of the cellular crosstalk within the liver. This is further implicated by the positive correlation of $ICOS^{high}CD8^+$ T cells with monocyte activation and the fact that the observed activation was particularly increased in the intermediate monocyte subset ($CD163^{high}CCR2^{high}$) in CPI-Hep, compared to CPI-noHep. Intermediate monocytes were shown to be predominantly pro-inflammatory and to express the highest levels of antigen presentation molecules and may therefore be more potent activators of $CD8^+$ T cells in CPI-Hep.[43–45]

Our study has a number of limitations. Firstly, immune phenotyping was limited to cells of monocyte and T cell lineage. However, other immune cells might play a role. Secondly, there was a degree of heterogeneity of treatment and tumour type among our patient cohort. For example, greater numbers of CPI-Hep patients were treated with combination CPI than CPI-noHep. Although, comparison of combination and single CPI treatment in CPI-Hep showed no differences in the reported phenotypic changed, the patient numbers were insufficient to do subgroup analyses of specific CPIs and tumour types or of the response rates to immunotherapy, though this has been addressed in larger cohorts.[46,47] In addition, the CPI-Hep group contained patients who had commenced corticosteroid treatment by the time of initial sampling. We mitigated the confounding effect of steroid treatment by selecting only steroid-naïve patients for gene expression analysis and comparisons of steroid-treated with naïve patients did not show significant differences in immunophenotyping. By concentrating our study on CPI-Hep patients, and due to the fact that CPI-noHep patients showed no development of other irAEs, we are unable to determine whether the peripheral changes we have described are common to all organ toxicities (irAEs) or specific to liver toxicity. Future work looking to replicate this phenotype in patients with different organ irAEs would be of value.

In conclusion, we have demonstrated an association between an activated peripheral monocyte phenotype and an expanded effector $CD8^+$ T cell population with liver toxicity in CPI-treated patients. Peripheral changes are mirrored in the liver where an inflammatory infiltrate characterised by co-localised $CD8^+$ T cells and $CCR2^+$ macrophages is demonstrated. A number of the pathways highlighted in this work have potential utility in disease monitoring and management as biomarkers. Though associative, these findings provide novel and important evidence regarding the immunopathogenesis of CPI-Hep and highlight future areas for research in this condition that is of increasing clinical consequence.

Abbreviations

ALF, acute liver failure; ALT, alanine transaminase; CAP, controlled attenuation parameter; CPI, immune checkpoint inhibitors; CPI-Hep, CPI-treatment with hepatic irAE; CPI-noHep, CPI-treatment without hepatic irAE; CTLA-4, cytotoxic T-lymphocyte antigen-4, *E. coli*, *Escherichia coli*; ELISA, enzyme-linked immunosorbent assay; HC, healthy controls; INR, international normalised ratio; irAEs, immune-related adverse events; LPS, lipopolysaccharide; LSM, liver stiffness measurement; MFI, mean fluorescence intensity; MoMF, monocyte-derived macrophages, PD-1, programmed cell death-1; PD-L1, programmed cell death ligand-1; PBMCs, peripheral blood mononuclear cells; ROS, reactive oxygen species; sCD163, Soluble CD163; Tregs, regulatory T cells.

Financial support

Royal Marsden Cancer Charity, Rosetree's Trust (A1783), Academy of Medical Sciences. Authors supported by UK NIHR and NIHR Imperial Biomedical Research Centre (BRC) and the Imperial College Wellcome Trust Strategic Fund.

Conflict of interest

The authors declare that the research was conducted in the absence of any commercial or financial relationships that could be construed as a potential conflict of interest.

Please refer to the accompanying ICMJE disclosure forms for further details.

Authors' contributions

Conceptualisation – CG, WK, CA, ST, LP. Investigation, Data curation, Formal analysis – CG, ET, TL. Interpretation of data – CG, ET, KW, RG, WK, CA, ST, LP. Resources and material support – LA, BS, RN, NK, SM, AD, YY, DP. Writing - original draft – CG, WK, LP. Writing - critical revision of manuscript – CG, MT, WK, ST, LP. Funding acquisition – MT, RG, MG, JL, WK, CA, ST, LP

Data availability statement

Data file available on Mendeley Data DOI: 10.17632/d5y3y9zhzn.1

Acknowledgements

The authors gratefully acknowledge all the patients that participated in the study. They thank the University College London Nanostring Facility for providing the nCounter system and related services, and St Mary's NHLI FACS core facility and Dr Yanping Guo for support and instrumentation. They also thank the Imperial Biomedical Research Council for infrastructure support and The Rosetrees Trust and the PEACE consortia for ongoing funding support. CG is funded by The Royal Marsden Cancer Charity and The Rosetrees Trust. LP is funded by an NIHR Clinical Lectureship and Academy of Medical Sciences Starter Grant. ST is funded by Cancer Research UK (grant reference number C50947/A18176), the National Institute for Health Research (NIHR) Biomedical Research Centre at the Royal Marsden Hospital and Institute of Cancer Research (grant reference number A109), the Kidney and Melanoma Cancer Fund of The Royal Marsden Cancer Charity, The Rosetrees Trust (grant reference number A2204), and Ventana Medical Systems Inc (grant reference numbers 10467 and 10530). ST has received speaking fees from Roche, Astra Zeneca, Novartis and Ipsen. DJP received funding from the Wellcome Trust Strategic Fund (PS3416) and infrastructural support from the Imperial College Tissue Bank. DJP received lecture fees from ViiV Healthcare, Roche, Bayer Healthcare and travel expenses from BMS and Bayer Healthcare; consulting fees for Mina Therapeutics, Roche, EISAI, Astra Zeneca and received research funding (to institution) from MSD, BMS. The graphical abstract was created using BioRender.com.

Supplementary data

Supplementary data to this article can be found online at https://doi.org/10.1016/j.jhep.2021.02.008.

References

Author names in bold designate shared co-first authorship

[1] Weber J. Immune checkpoint proteins: a new therapeutic paradigm for cancer—preclinical background: CTLA-4 and PD-1 blockade. Semin Oncol 2010;37:430–439.
[2] Fessas P, Possamai LA, Clark J, Daniels E, Gudd C, Mullish BH, et al. Immunotoxicity from checkpoint inhibitor therapy: clinical features and underlying mechanisms. Immunology 2020;159:167–177.
[3] Larkin J, Chiarion-Sileni V, Gonzalez R, Grob J-J, Rutkowski P, Lao CD, et al. Five-year survival with combined nivolumab and ipilimumab in advanced melanoma. N Engl J Med 2019;381:1535–1546.
[4] Hellmann MD, Ciuleanu TE, Pluzanski A, Lee JS, Otterson GA, Audigier-Valette C, et al. Nivolumab plus ipilimumab in lung cancer with a high tumor mutational burden. N Engl J Med 2018;378:2093–2104.
[5] **El-Khoueiry AB**, **Sangro B**, Yau T, Crocenzi TS, Kudo M, Hsu C, et al. Nivolumab in patients with advanced hepatocellular carcinoma (CheckMate 040): an open-label, non-comparative, phase 1/2 dose escalation and expansion trial. Lancet 2017;389:2492–2502.
[6] Schmid P, Rugo HS, Adams S, Schneeweiss A, Barrios CH, Iwata H, et al. Atezolizumab plus nab-paclitaxel as first-line treatment for unresectable, locally advanced or metastatic triple-negative breast cancer (IMpassion130): updated efficacy results from a randomised, double-blind, placebo-controlled, phase 3 trial. Lancet Oncol 2020;21:44–59.
[7] Nghiem PT, Bhatia S, Lipson EJ, Kudchadkar RR, Miller NJ, Annamalai L, et al. PD-1 blockade with pembrolizumab in advanced Merkel-cell carcinoma. N Engl J Med 2016;374:2542–2552.
[8] Overman MJ, McDermott R, Leach JL, Lonardi S, Lenz H-J, Morse MA, et al. Nivolumab in patients with metastatic DNA mismatch repair-deficient or microsatellite instability-high colorectal cancer (CheckMate 142): an open-label, multicentre, phase 2 study. Lancet Oncol 2017;18:1182–1191.
[9] Ansell SM, Lesokhin AM, Borrello I, Halwani A, Scott EC, Gutierrez M, et al. PD-1 blockade with nivolumab in relapsed or refractory Hodgkin's lymphoma. N Engl J Med 2014;372:311–319.
[10] Hammers HJ, Plimack ER, Infante JR, Rini BI, McDermott DF, Lewis LD, et al. Safety and efficacy of nivolumab in combination with ipilimumab in metastatic renal cell carcinoma: the CheckMate 016 study. J Clin Oncol 2017;35:3851–3858.
[11] De Martin E, Michot JM, Papouin B, Champiat S, Mateus C, Lambotte O, et al. Characterization of liver injury induced by cancer immunotherapy using immune checkpoint inhibitors. J Hepatol 2018;68:1181–1190.
[12] Postow MA, Sidlow R, Hellmann MD. Immune-related adverse events associated with immune checkpoint blockade. N Engl J Med 2018;378:158–168.
[13] Haanen JBAG, Carbonnel F, Robert C, Kerr KM, Peters S, Larkin J, et al. Management of toxicities from immunotherapy: ESMO Clinical Practice Guidelines for diagnosis, treatment and follow-up. Ann Oncol 2017;28:iv119–iv142.
[14] Brahmer JR, Lacchetti C, Schneider BJ, Atkins MB, Brassil KJ, Caterino JM, et al. Management of immune-related adverse events in patients treated with immune checkpoint inhibitor therapy: American Society of Clinical Oncology Clinical Practice Guideline. J Clin Oncol – Off J Am Soc Clin Oncol 2018;36:1714–1768.
[15] Huppert LA, Gordan JD, Kelley RK. Checkpoint inhibitors for the treatment of advanced hepatocellular carcinoma. Clin Liver Dis 2020;15:53–58.
[16] Karlmark KR, Weiskirchen R, Zimmermann HW, Gassler N, Ginhoux F, Weber C, et al. Hepatic recruitment of the inflammatory Gr1+ monocyte subset upon liver injury promotes hepatic fibrosis. Hepatology 2009;50:261–274.
[17] Antoniades CG, Quaglia A, Taams LS, Mitry RR, Hussain M, Abeles R, et al. Source and characterization of hepatic macrophages in acetaminophen-induced acute liver failure in humans. Hepatology 2012;56:735–746.
[18] Mossanen JC, Krenkel O, Ergen C, Govaere O, Liepelt A, Puengel T, et al. Chemokine (C-C motif) receptor 2–positive monocytes aggravate the early phase of acetaminophen-induced acute liver injury. Hepatology 2016;64:1667–1682.
[19] Krenkel O, Puengel T, Govaere O, Abdallah AT, Mossanen JC, Kohlhepp M, et al. Therapeutic inhibition of inflammatory monocyte recruitment reduces steatohepatitis and liver fibrosis. Hepatology 2018;67:1270–1283.
[20] McElroy AK, Shrivastava-Ranjan P, Harmon JR, Martines RB, Silva-Flannery L, Flietstra TD, et al. Macrophage activation marker soluble CD163 associated with fatal and severe Ebola virus disease in humans. Emerg Infect Dis 2019;25:290–298.
[21] Ye H, Wang LY, Zhao J, Wang K. Increased CD163 expression is associated with acute-on-chronic hepatitis B liver failure. World J Gastroenterol 2013;19:2818–2825.
[22] Andersen ES, Rødgaard-Hansen S, Moessner B, Christensen PB, Møller HJ, Weis N. Macrophage-related serum biomarkers soluble CD163 (sCD163) and soluble mannose receptor (sMR) to differentiate mild liver fibrosis from cirrhosis in patients with chronic hepatitis C: a pilot study. Eur J Clin Microbiol Infect Dis 2014;33:117–122.
[23] Burdo TH, Lo J, Abbara S, Wei J, DeLelys ME, Preffer F, et al. Soluble CD163, a novel marker of activated macrophages, is elevated and associated with noncalcified coronary plaque in HIV-infected patients. J Infect Dis 2011;204:1227–1236.
[24] Vergis N, Khamri W, Beale K, Sadiq F, Aletrari MO, Moore C, et al. Defective monocyte oxidative burst predicts infection in alcoholic hepatitis and is associated with reduced expression of NADPH oxidase. Gut 2017;66:519–529.
[25] Triantafyllou E, Pop OT, Possamai LA, Wilhelm A, Liaskou E, Singanayagam A, et al. MerTK expressing hepatic macrophages promote the resolution of inflammation in acute liver failure. Gut 2018.
[26] Bernsmeier C, Triantafyllou E, Brenig R, Lebosse FJ, Singanayagam A, Patel VC, et al. $CD14^+$ $CD15^-$ $HLA\text{-}DR^-$ myeloid-derived suppressor cells

impair antimicrobial responses in patients with acute-on-chronic liver failure. Gut 2018;67:1155–1167.
[27] Foureau DM, Walling TL, Maddukuri V, Anderson W, Culbreath K, Kleiner DE, et al. Comparative analysis of portal hepatic infiltrating leucocytes in acute drug-induced liver injury, idiopathic autoimmune and viral hepatitis. Clin Exp Immunol 2015;180:40–51.
[28] Metushi IG, Hayes MA, Uetrecht J. Treatment of PD-1(-/-) mice with amodiaquine and anti-CTLA4 leads to liver injury similar to idiosyncratic liver injury in patients. Hepatology 2015;61:1332–1342.
[29] Mak A, Uetrecht J. Involvement of CCL2/CCR2 macrophage recruitment in amodiaquine-induced liver injury. J Immunotoxicol 2019;16:28–33.
[30] Fujimura T, Sato Y, Tanita K, Kambayashi Y, Otsuka A, Fujisawa Y, et al. Serum levels of soluble CD163 and CXCL5 may be predictive markers for immune-related adverse events in patients with advanced melanoma treated with nivolumab: a pilot study. Oncotarget 2018;9:15542–15551.
[31] Chiang EY, Johnston RJ, Grogan JL. EBI2 is a negative regulator of type I interferons in plasmacytoid and myeloid dendritic cells. PLoS One 2013;8:e83457.
[32] Mahnke YD, Brodie TM, Sallusto F, Roederer M, Lugli E. The who's who of T-cell differentiation: human memory T-cell subsets. Eur J Immunol 2013;43:2797–2809.
[33] Espert L, Degols G, Gongora C, Blondel D, Williams BR, Silverman RH, et al. ISG20, a new interferon-induced RNase specific for single-stranded RNA, defines an alternative antiviral pathway against RNA genomic viruses. J Biol Chem 2003;278:16151–16158.
[34] Hao Y, Yang D. Cloning, eukaryotic expression of human ISG20 and preliminary study on the effect of its anti-HBV. J Huazhong Univ Sci Technol Med Sci 2008;28:11–13.
[35] Jiang D, Guo H, Xu C, Chang J, Gu B, Wang L, et al. Identification of three interferon-inducible cellular enzymes that inhibit the replication of hepatitis C virus. J Virol 2008;82:1665–1678.
[36] **Nish SA**, **Schenten D**, **Wunderlich FT**, Pope SD, Gao Y, Hoshi N, et al. T cell-intrinsic role of IL-6 signaling in primary and memory responses. Elife 2014;3:e01949.
[37] Gu JJ, Stegmann S, Gathy K, Murray R, Laliberte J, Ayscue L, et al. Inhibition of T lymphocyte activation in mice heterozygous for loss of the IMPDH II gene. J Clin Invest 2000;106:599–606.
[38] Cruz-Munoz M-E, Dong Z, Shi X, Zhang S, Veillette A. Influence of CRACC, a SLAM family receptor coupled to the adaptor EAT-2, on natural killer cell function. Nat Immunol 2009;10:297–305.
[39] Joller N, Hafler JP, Brynedal B, Kassam N, Spoerl S, Levin SD, et al. Cutting edge: TIGIT has T cell-intrinsic inhibitory functions. J Immunol 2011;186:1338–1342.
[40] Cevik SI, Keskin N, Belkaya S, Ozlu MI, Deniz E, Tazebay UH, et al. Cd81 interacts with the T cell receptor to suppress signaling. PLoS One 2012;7:e50396.
[41] Brownlie RJ, Wright D, Zamoyska R, Salmond RJ. Deletion of PTPN22 improves effector and memory CD8+ T cell responses to tumors. JCI Insight 2019;4:e127847.
[42] Takata H, Naruto T, Takiguchi M. Functional heterogeneity of human effector CD8+ T cells. Blood 2012;119:1390–1398.
[43] Wong KL, Yeap WH, Tai JJY, Ong SM, Dang TM, Wong SC. The three human monocyte subsets: implications for health and disease. Immunol Res 2012;53:41–57.
[44] Wong KL, Tai JJ-Y, Wong W-C, Han H, Sem X, Yeap W-H, et al. Gene expression profiling reveals the defining features of the classical, intermediate, and nonclassical human monocyte subsets. Blood 2011;118:e16–e31.
[45] Lee J, Tam H, Adler L, Ilstad-Minnihan A, Macaubas C, Mellins ED. The MHC class II antigen presentation pathway in human monocytes differs by subset and is regulated by cytokines. PLoS One 2017;12:e0183594.
[46] Rogado J, Sánchez-Torres JM, Romero-Laorden N, Ballesteros AI, Pacheco-Barcia V, Ramos-Leví A, et al. Immune-related adverse events predict the therapeutic efficacy of anti-PD-1 antibodies in cancer patients. Eur J Cancer 2019;109:21–27.
[47] Okada N, Kawazoe H, Takechi K, Matsudate Y, Utsunomiya R, Zamami Y, et al. Association between immune-related adverse events and clinical efficacy in patients with melanoma treated with nivolumab: a multicenter retrospective study. Clin Ther 2019;41:59–67.